Design and Implementation of a Laboratory Course for UWB-Based Positioning via Two-Way Ranging with Kalman Filter Data Fusion

Natalia Skliar[2,*], *Aleksandr* Khelvas[1,3,**], *Roman* Kostin[1,3,***], *Aleksandr* Gilya-Zetinov[1,****], *Ali* Alizadeh[1,†], *Albert* Danilov[1,‡], *Abuk* Saidov[1,3,§], *Dmitry* Severov[1,3,¶], *Ruslan* Pashkov[1,3,‖], *Mikhail* Marinovich[1,3,**], and *Roman* Pavlovich[4,††]

[1]Moscow Institute of Physics and Technologies, Moscow, Russian Federation
[2]National Research University Higher School of Economics
[3]SOCCOS LLC, Moscow, Russian Federation
[4]AtFrame DOO, NoviSad, Republic of Serbia

Abstract. This article presents an original solution for a laboratory work on the application of Two Way Ranging Ultra-Wide Band positioning methods, designed for courses in technical universities and institutes. The laboratory work is aimed at providing students with a comprehensive understanding of the interaction between the hardware of distributed Ultra-Wide Band Two Way Ranging navigation measurement systems and data processing algorithms based on Kalman filtering.
Keywords: Kalman filters, Indoor Positioning, Ultra-Wide Band, Kalman filter, Two Way Ranging, Internet of Things

1 Introduction

The purpose of this laboratory work is to familiarize students with the principles of object positioning based on Ultra-Wideband (UWB) technology and to master the methods of processing multidimensional measurements using the Kalman filter. Within the framework of this work, students will use a practical example to study how the results of physical measurements are combined with mathematical models to improve the accuracy of real-time coordinate determination.

To successfully complete the laboratory work, students need to have basic knowledge in the field of linear algebra, probability theory, programming in the Python language, as well as

[*]e-mail: natalyasklyar.05@gmail.com
[**]e-mail: hel@cos.ru
[***]e-mail: rqk@stlport.com
[****]e-mail: entuser@yandex.ru
[†]e-mail: ali.rim.alizadeh@phystech.edu
[‡]e-mail: danilov@cos.ru
[§]e-mail: abuk.saidov@azimut.ru
[¶]e-mail: dseverov@mail.mipt.ru
[‖]e-mail: ruslan.pashkoff@gmail.com
[**]e-mail: marinovich.ml@phystech.edu
[††]e-mail: prv@atframe.rs

the fundamentals of radio engineering systems (the principle of measuring distance by signal delay).

As a result of the work, students will acquire practical skills in:

1. working with UWB-based measurement equipment;
2. conducting a series of experiments on distance measurement and their statistical processing;
3. formulating and testing hypotheses about the distribution of measurement errors;
4. applying a multidimensional Kalman filter for filtering and predicting object coordinates;
5. evaluating the accuracy of positioning methods.

The laboratory work is aimed at forming a holistic understanding among students about the interaction of the hardware part of measurement systems and data processing algorithms.

2 Basics of UWB

This research is based on Ultra-Wideband (UWB) technology, a method of wireless data transmission characterized by a number of fundamental features. A key distinguishing trait of UWB is the utilization of an extremely wide frequency bandwidth (with an absolute width exceeding 500 MHz) within the range of 3.1 to 10.6 GHz. This approach, in contrast to the use of high-amplitude narrowband signals, involves the emission of signals with an extremely low power spectral density (less than -35 dBm/MHz). This ensures resistance to interference and allows this technology to coexist with other wireless systems. [1]

UWB technology supports data rates ranging from 110 kbps to 6.8 Mbps over distances of up to 200 meters. However, its most significant property for the purposes of this study is the capability for high-precision ranging (distance measurement) between devices, with a potential accuracy on the order of 0.1 meters. [2] This capability is realized because the wideband signal allows for highly precise detection of the time of arrival of pulses.

This research employs a hardware platform based on the DW1000 transceiver manufactured by Decawave (now Qorvo). [3] The specified chip is a half-duplex wireless transceiver operating in the frequency range from 3.2 to 7.5 GHz and featuring software-controlled transmit power. The maximum supported data rate for this chip is 6.8 Mbps.

A critically important component of the DW1000 integrated circuit for precision timing applications is its built-in 40-bit hardware timer/counter. Its value range extends from 0 to $2^4$0 (1,099,511,627,776 discrete counts). The clock frequency governing the increment of this timer is 64 GHz, which results in an extremely high temporal resolution of the system: the timer value increases by one every 15.625 picoseconds (ps). During this time interval, electromagnetic radiation travels approximately 4.687 millimeters in free space (considering the speed of light 3×10^8 m/s). The period of a full timer overflow, i.e., the time it takes for its value to complete a full cycle from 0 to 2^{40}, is approximately 17.17 seconds.

The principle of measuring the distance between two objects, implemented in this work, requires at least two transceivers capable of alternately transmitting and receiving data packets. The essence of the method lies in the precise recording of timestamps for the moment a packet is sent by one device and the moment it is received by a second device. The difference between these timestamps, proportional to the signal's time of flight, forms the basis for the subsequent calculation of distance.

In UWB-based positioning systems, devices perform different roles. [4]

Tag is the initiating device, which is typically mobile and moves through space.

Anchor is a stationary device that receives and responds to requests from the Tag. The object's position is determined based on the measured signal delays from several Anchors.

Listener (Node) is a device that does not participate in the direct exchange but "listens" to the radio traffic and transmits the collected packets to an external computing system for subsequent processing.

This distribution of roles enables the construction of scalable tracking systems where mobile objects interact with a fixed infrastructure.

UWB Single Sided Two-Way Ranging (SS-TWR) is a method for determining the distance between two devices using UWB communication technology (fig.1). [3] It is based on measuring the round-trip time of a radio signal (from the Tag device to the Anchor device and back) using two main signals with four timestamps. The SS-TWR method has relatively low measurement accuracy due to the influence of instability in the crystal oscillators of the devices. To improve accuracy and compensate for this instability when using UWB transceivers, DS-TWR technology is employed.

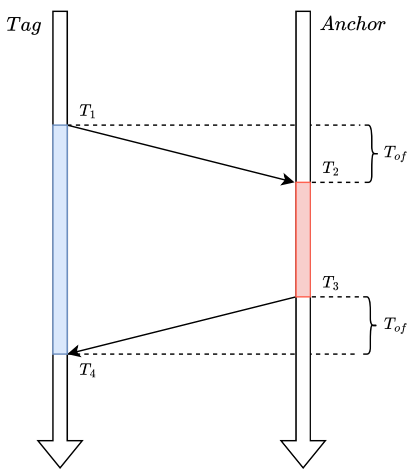

Figure 1. SS-TWR

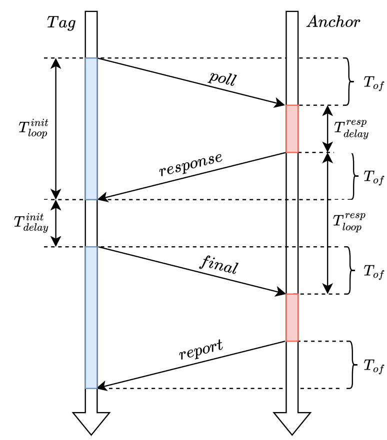

Figure 2. DS-TWR

UWB Double-Sided Two-Way Ranging (DS-TWR) is an enhanced version of the SS-TWR algorithm that uses two rounds of message exchange between devices (instead of one in SS-TWR) with three main signals and six timestamps (fig.2). [3] This minimizes the contribution of clock error on each device to the final estimate of the signal propagation time.

In the case of SS-TWR, the distance between the tag and the anchor (L) is calculated using the formulas:

$$L = c \cdot T_{of} = c \cdot \frac{1}{2}(T_{round} - T_{reply}) = c \cdot \frac{1}{2}(T_4 - T_1 - T_3 + T_2) \tag{1}$$

where c is the speed of light.

The times T_{round} and T_{reply} are measured independently on the tag and the anchor using their own crystal oscillators, which have their own deviations from the nominal frequency. Consequently, the final estimate of the time T_{of} contains an error that increases with increasing T_{reply}.

For DS-TWR, the formula for calculating the distance (L), taking into account compensation for the instability of the crystal oscillator frequency, is as follows:

$$L = c \cdot T_{\text{fly}} = c \cdot \frac{T_{\text{loop}}^{\text{init}} \cdot T_{\text{loop}}^{\text{resp}} - T_{\text{delay}}^{\text{init}} \cdot T_{\text{delay}}^{\text{resp}}}{T_{\text{loop}}^{\text{init}} + T_{\text{loop}}^{\text{resp}} + T_{\text{delay}}^{\text{init}} + T_{\text{delay}}^{\text{resp}}} \tag{2}$$

where c is the speed of light.

The device initiating the TWR session in the work is called a tag. Typically, the tag is mobile. The UWB transceiver that listens for and responds to messages from the tag is called an anchor. Anchors are usually stationary. The UWB receiver that only listens to the airwaves and sends received packets for further processing to an external computing system is called a listener or sometimes referred to as a node in other literature. Listeners are also stationary.

3 State of the Art

3.1 UWB in Indoor Positioning Systems

The problem we are solving belongs to the class of tasks involving tracking moving objects and determining their location indoors.

Thanks to significant progress in electronics and communication systems, technologies for precise positioning inside buildings have emerged—so-called Indoor Positioning Systems (IPS). Among these, Ultra-Wideband (UWB) technology holds a special place. It offers a number of advantages compared to other solutions: it provides secure and robust communication, has a wide bandwidth, high data transfer rate, and low power consumption. The growing need for indoor localization lacks a universal standard, requiring system selection based on the specific environment and accuracy needs. This paper surveys various techniques like RSSI, TOA, TDoA, and AOA.

It categorizes systems as active (requiring a tag or device) or passive (requiring no carried device). The survey [5] evaluates and compares these systems based on criteria such as technology, algorithms, accuracy, complexity, scalability, and cost, outlining their respective advantages and disadvantages.

The article [6] provides a review of state-of-the-art, as of 2024, real-time systems for tracking and localizing moving objects based on UWB. The authors analyze the latest UWB modules and solutions available on the market, as well as different types of algorithms used for high-precision positioning.

The article [7] investigates the fundamentals of UWB interoperability. The authors have prepared a review of various UWB radio chips available on the market. This is followed by an overview of existing UWB standards and the organizations that support these standards. The authors describe interoperability challenges and related aspects of interaction at the physical layer (PHY), medium access control layer (MAC), and higher layers.

The article [2] covers the current state of the UWB standards.

The hardware solution QORVO DW1001 used in our experiments was developed by Decawave. Documentation for the DWM1001 (SW-DWM1001-Firmware-User-Guide-1.4) is available on the QORVO website [3].

The paper [8] details the development and testing of a low-cost, UWB Real-Time Locating System using the commercial Qorvo MDEK1001 kit. The system tracks tags within an area covered by fixed anchors.

Tests conducted in both a lab and a real industrial environment showed promising results for tracking assets. Crucially, the economic analysis confirms the system is a viable, low-cost investment, making it particularly suitable for small and medium-sized enterprises. The paper serves as a practical guide for implementing such a system.

A feature of UWB-based positioning systems is the need for continuous accounting and compensation of various types of errors. One way to improve the quality of object coordinate determination is the use of motion models combined with filtering algorithms. A common approach is Kalman filtering. For example, the article [9] proposes an indoor positioning system using UWB technology and a modified Kalman filter. The system includes several embedded hardware devices for transmitting and receiving UWB data, applies a Kalman filter to reduce signal noise and improve accuracy, and a software stack for calculating position using the Time Difference of Arrival (TDOA) method and a trilateration algorithm, followed by data storage.

The work [10] proposes an enhanced UWB positioning system based on two-dimensional trilateration, where a Kalman filter algorithm is used to eliminate errors and drift of positioning points caused by the robot's operational characteristics, significantly improving the accuracy of auxiliary positioning.

The work [11] addresses the problem of UWB devices being susceptible to interference and the associated positioning errors. To solve this problem, a Kalman filter is first applied to process the distance measurement data to eliminate erroneous values caused by noise interference. Then, a Gaussian filter is used to improve the accuracy of distance measurements. Next, initial coordinates are calculated using the Chan algorithm, after which these coordinates are used as initial search values in an enhanced particle swarm optimization algorithm to obtain more accurate coordinate values. The positioning accuracy of the algorithm is evaluated using the Root Mean Square Error (RMSE).

Modern research shows that artificial intelligence (AI) algorithms can improve UWB positioning accuracy by processing large volumes of data.

The work [12] presents a review of challenges and their AI-based solutions in UWB localization systems, along with an analysis of existing research and a practical application example.

3.2 Theoretical Foundations of the Kalman Filter

The Kalman filter is a recursive algorithm for estimating the state of a dynamic system based on a series of noisy measurements [13]. The main task of the Kalman filter is to correctly estimate the state of the system, taking into account both measurement noise and process noise.

For a system with linear dynamics, the state is described by the vector $\mathbf{x}_k$ and evolves according to the model

$$\mathbf{x}_{k|k-1} = F\mathbf{x}_{k-1} + \mathbf{w}_{k-1}, \quad \mathbf{w}_{k-1} \sim \mathcal{N}(0, Q),$$

where F is the state transition matrix, w is the Gaussian process noise with covariance Q. The system measurements are represented as

$$\mathbf{z}_k = h(\mathbf{x}_k) + \mathbf{v}_k, \quad \mathbf{v}_k \sim \mathcal{N}(0, R),$$

where $\mathbf{v}_k$ is the Gaussian measurement noise with covariance R, and the function $h(\mathbf{x})$ describes the dependence of the observed quantities on the system state.

The Kalman filter operates recursively in two stages:

1. Prediction -— a priori estimation of the state and error covariance based on the motion model;

2. Update —- updating the state and covariance based on new measurements.

In the case of nonlinear dynamics and/or measurements, the Extended Kalman Filter (EKF) is applied, in which the functions h and F are linearized using Jacobians relative to the current state estimate.

4 Methods and Materials

The equipment includes DevKit boards flashed with the SOCCOS.UWB firmware, which allows the boards to be configured as a Tag, Anchor, or Listener.

The first lab focuses on distance measurement between two devices, both of which are connected to a personal computer running Windows or Linux (fig.3).

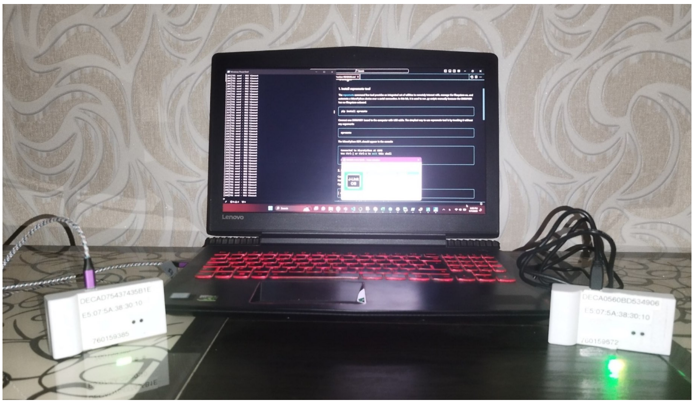

Figure 3. Laboratory Equipment Set for Laboratory 1

In this laboratory work, experiments are conducted in a specially equipped classroom. The room is equipped with four Anchors installed in the corners in such a way that they form a geometric configuration close to a tetrahedron (fig.4). Each student group is provided with one Tag and one Listener connected to a personal computer.

Each Tag exchanges messages with all four Anchors in the classroom using the DS-TWR protocol. The Listener receives all packets circulating in the network and transmits them to the computer in the form of binary logs.

At the processing stage, the data can be filtered for a specific Tag. For the selected device, distances to each of the Anchors are calculated based on the timestamps of transmitted and received messages. These measurements are used for subsequent object localization.

5 Laboratories description

5.1 Distance Measurement Between Two UWB Modules

The experiment involves measuring distances between two UWB trackers: *anchor* (stationary receiver) and *tag* (mobile transmitter) at regular time intervals.

Due to the inaccuracy of measuring instruments, the data is noisy. To address this issue, the Extended Kalman Filter (EKF) method is used. The main goal is to remove noise associated with measurement errors while preserving process noise.

The system state is described by the vector:

$$\mathbf{x} = \begin{bmatrix} x \\ v_x \end{bmatrix}, \tag{3}$$

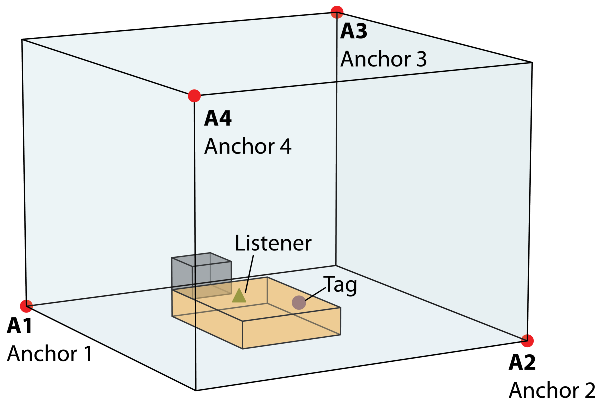

Figure 4. Laboratory Equipment Set for Laboratory 2

where x is the tag's coordinate along the x-axis, and v_x is its velocity.

The state transition model over time Δt is given by the motion equation:

$$\mathbf{x}_{k|k-1} = F\mathbf{x}_{k-1}, \quad F = \begin{bmatrix} 1 & \Delta t \\ 0 & 1 \end{bmatrix}. \tag{4}$$

The prediction covariance matrix is updated using the formula:

$$P_{k|k-1} = FP_{k-1}F^{\top} + Q, \tag{5}$$

where Q is the process noise covariance matrix.

The distance measurement between the tag and anchor:

$$z_k = h(\mathbf{x}_k) = |x_k + \Delta t \cdot v_{x,k} - x_a|, \tag{6}$$

where x_a is the coordinate of the stationary anchor.

The Jacobian of the measurement function:

$$H_k = \begin{bmatrix} \dfrac{x_k + \Delta t \cdot v_{x,k} - x_a}{|x_k + \Delta t \cdot v_{x,k} - x_a| + \varepsilon} & 0 \end{bmatrix}, \tag{7}$$

where ε is a small positive number close to zero to avoid division by zero.

The measurement prediction error and its covariance:

$$\mathbf{y}_k = z_k - h(\mathbf{x}_{k|k-1}), \tag{8}$$

$$S_k = H_k P_{k|k-1} H_k^{\top} + R, \tag{9}$$

where R is the measurement noise variance.

The Kalman gain:

$$K_k = P_{k|k-1} H_k^{\top} S_k^{-1}. \tag{10}$$

State and covariance update:

$$\mathbf{x}_k = \mathbf{x}_{k|k-1} + K_k \mathbf{y}_k, \tag{11}$$

$$P_k = (I - K_k H_k) P_{k|k-1}. \tag{12}$$

With each new measurement, the state prediction and value correction are performed. As a result, a more accurate picture of the object's real trajectory is obtained.

Initialization

Before starting the filter, the following parameters are set:

1. initial state $\mathbf{x}_0$ (first measurement and zero velocity);
2. initial covariance $P_0 = 100 \cdot I$;
3. noise parameters Q and R, reflecting the nature of motion and measurement instrument accuracy;
4. anchor coordinate x_a.

Implementation on Real Data

To demonstrate the filter's operation, it was run on real data from trackers.

The filter was configured with the following parameters:

1. time discretization step: $dt = 0.1$ s;
2. process noise variance: $q = 0.01$;
3. measurement noise variance: $r = 10.0$;
4. initial state: $x_0 = 0.0$ m, $v_{x0} = 0.1$ m/s;
5. anchor position: $x_{\text{anchor}} = 0.0$ m.

The log file contains measurements between the "anchor" and "tag" at regular time intervals.

For each measurement, the following steps are performed:

1. Prediction step , where the filter updates the a priori state estimate and error covariance;
2. Correction step, where the a posteriori state estimate is updated using the new measurement.

As a result of the filter's operation, trajectories of the estimated tag position and velocity were obtained.

5.2 Three-Dimensional Navigation Relative to a Set of UWB Anchors

To obtain the complete trajectory of an object's motion in space, an Extended Kalman Filter (EKF) in three-dimensional space is used. In this case, measurements are received simultaneously from three anchors, and the tag moves in (x, y, z) space.

The goal is to estimate the position and velocity of the tag in three-dimensional space based on distance measurements to UWB anchors (fig.6). For the sake of simplicity, in this section, all the equations are provided for the case of three anchors instead of four. Assuming the tag moves exclusively within one half-space (for example, only upward and to the right), three anchors are sufficient to unambiguously determine the tag's position. Unlike the 1D case, the EKF is employed not only to mitigate measurement noise, but also to solve the trilateration problem and derive coordinates from the distances between the tag and the anchors.

Let at each Δt (discretization step) the following data be received:

r_i^t — distance from the tag to the i-th anchor, $i = 1, 2, 3$;

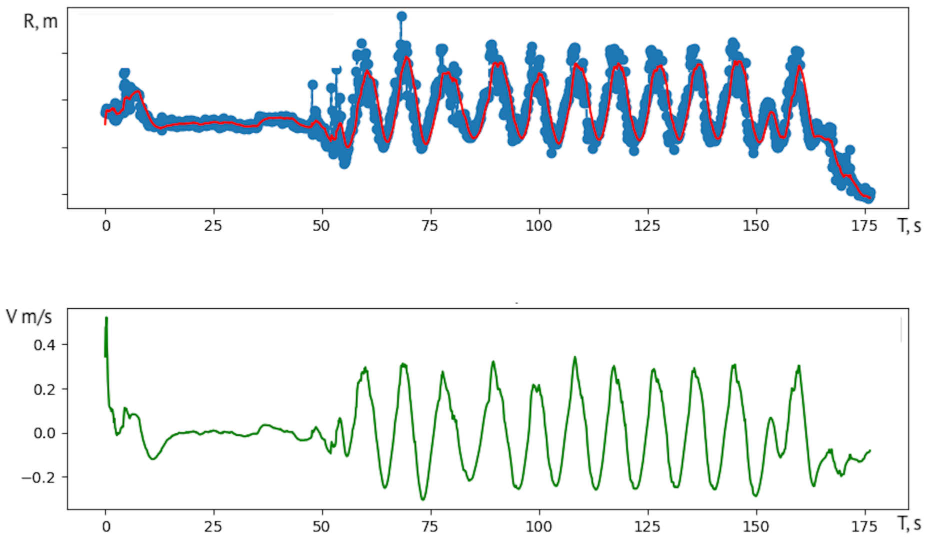

Figure 5. EKF filtering results: a) comparison of measured distances and filter estimates; b) tag velocity estimate.

$\mathbf{p}_i = (x_i, y_i, z_i)$ — coordinates of the i-th anchor.
The system state is defined as

$$\mathbf{x}_t = [x, y, z, v_x, v_y, v_z]^T$$

The state transition formula is:

$$\mathbf{x}_{t+1} = \mathbf{F}\mathbf{x}_t + \mathbf{w}_t$$

where $\mathbf{w}_t \sim \mathcal{N}(0, \mathbf{Q})$ is Gaussian noise, and the matrix $\mathbf{F}$ is:

$$\mathbf{F} = \begin{bmatrix} 1 & 0 & 0 & \Delta t & 0 & 0 \\ 0 & 1 & 0 & 0 & \Delta t & 0 \\ 0 & 0 & 1 & 0 & 0 & \Delta t \\ 0 & 0 & 0 & 1 & 0 & 0 \\ 0 & 0 & 0 & 0 & 1 & 0 \\ 0 & 0 & 0 & 0 & 0 & 1 \end{bmatrix}$$

The measurements consist of a vector of distances to the anchors:

$$\mathbf{z}_t = [r_1^t, r_2^t, r_3^t]^T = h(\mathbf{x}_t) + \mathbf{v}_t$$

where $\mathbf{v}_t \sim \mathcal{N}(0, \mathbf{R})$ is measurement noise, and the function h is:

$$h(\mathbf{x}_t) = \begin{bmatrix} \sqrt{(x - x_1)^2 + (y - y_1)^2 + (z - z_1)^2} \\ \sqrt{(x - x_2)^2 + (y - y_2)^2 + (z - z_2)^2} \\ \sqrt{(x - x_3)^2 + (y - y_3)^2 + (z - z_3)^2} \end{bmatrix}$$

The filtering process consists of state and covariance prediction and update based on new measurements. For this purpose, the Jacobian of function h with respect to the state ($\mathbf{H}_t$) is computed at each time step.

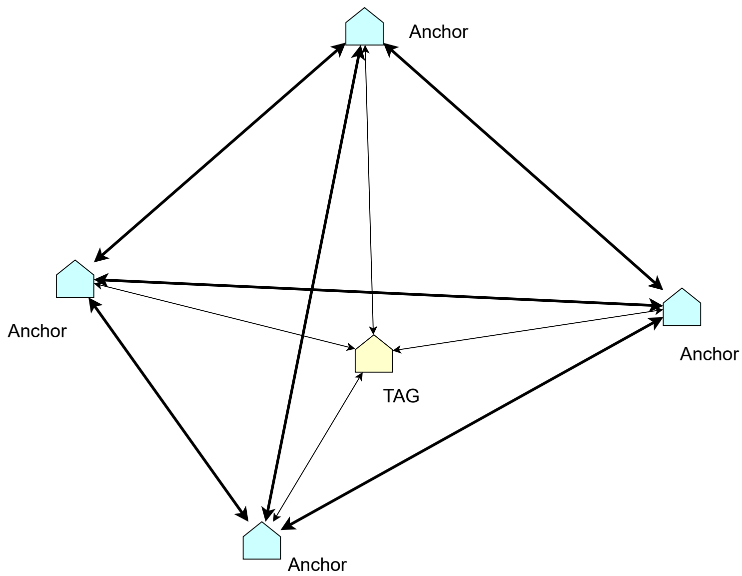

Figure 6. 3D Tag positioning

The Jacobian $\mathbf{H}_t = \frac{\partial h}{\partial \mathbf{x}}$ is calculated as:

$$\mathbf{H}_t = \begin{bmatrix} (x - x_1)/r_1 & (y - y_1)/r_1 & (z - z_1)/r_1 & 0 & 0 & 0 \\ (x - x_2)/r_2 & (y - y_2)/r_2 & (z - z_2)/r_2 & 0 & 0 & 0 \\ (x - x_3)/r_3 & (y - y_3)/r_3 & (z - z_3)/r_3 & 0 & 0 & 0 \end{bmatrix};$$

where $r_i = \sqrt{(x - x_i)^2 + (y - y_i)^2 + (z - z_i)^2}$.

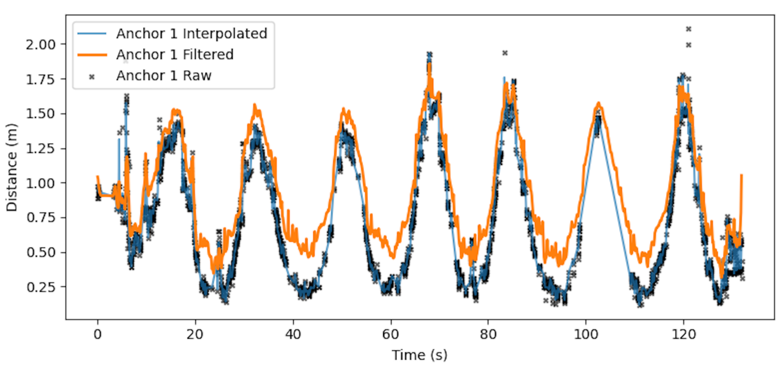

Figure 7. Distance from Tag to Anchor example

6 Measurement accuracy

The accuracy of distance measurements in UWB systems is limited by several factors. The main sources of errors in the obtained reception timestamps are:

1. Clock drift in tags and anchors;

2. Temporal bias in calculated first-path arrival time due to various factors, such as the received signal power level (RSL) and frequency difference (unrelated directly to the timestamps, but still affecting the result of DW1000's FP detection algorithm [14]);

3. Multipath propagation and reflections of signals indoors, which distort the actual signal's time-of-flight;

Each of these errors are modeled in different ways. In the literature, the commonly used approaches are:

1. The impact of clock drift, after compensating for the frequency difference by DS-TWR ranging method, is commonly approximated by a zero-mean Gaussian random variable. [15]

2. The offset introduced by the signal power level and the difference in frequency is compensated by an empirical lookup table or a fitted curve. [16]

3. The multipath presence is usually modeled by an additional, non-zero-mean Gaussian random variable with a variance different from that of the purely LOS case, and with the distribution parameters depending on particular environment and location. [15]

While more sophisticated filtering algorithms, such as RACKF, help to suppress the reflection-induced errors, we suggested EKF as a simpler starting point for course students to work with. The application of EKF with proper parameters is sufficient to suppress the zero-mean Gaussian random variable part of the error, and is able to achieve 4cm accuracy in good conditions. [17] To mitigate the rest of the error sources, in the proposed laboratory course, we recommend to minimize the amount of reflectors, such as large metallic objects and individuals in the laboratory area. Additionally, to keep the bias error due to signal strength low, we recommend keeping a minimum distance of 1 meter between anchors and a tag.

The error sources listed above affect the measured time-of-flight value. The time-of-flight measurement error δT translates into distance error δL:

$$\delta L = c \cdot \delta T, \tag{13}$$

where c is the speed of light.

The calculated distances are converted to coordinates by application of EKF, which effictively solves the trilateration task to determine a tag's coordinates. The resulting position error is connected to the ranging error through a well-studied concept of dilution of precision (DOP). [18] Usually, three types of DOP coefficients are introduced: horiozontal dilution (HDOP), vertical dilution (VDOP), and position diliution (PDOP) of precision. Each DOP coefficient is a coefficient of proportionality between the ranging error and the absolute positioning error or its projections:

$$PDOP = \frac{\sqrt{\sigma_x^2 + \sigma_y^2 + \sigma_z^2}}{\sigma_R}; \quad HDOP = \frac{\sqrt{\sigma_x^2 + \sigma_y^2}}{\sigma_R}; \quad VDOP = \frac{\sigma_z}{\sigma_R} \tag{14}$$

where σ_R is the standard deviation of ranging error, σ_x, σ_y, σ_z are the standard deviations of positioning error along different axes.

The DOP value depends greatly both on the anchor placement and the tag's position. [19] The accuracy degrades sharply when the tag is moved outside of the perimeter of the anchors' rectangle. Also, the optimal configuration of anchors shouldn't have coplanar anchors, otherwise the positioning errors notably increase when the tag is in the same plane, and are generally bigger in the direction of the plane's normal vector. The configuration suggested in this laboratory course (fig. 4) follows the general recommendations of the low-3D-error configurations in the work [20], and the expected PDOP value inside the anchor's rectangle lies in the 2–3 range.

To determine the actual accuracy in the presence of these errors, we have performed a series of controlled measurements in the proposed experimental setup.

First, we conducted a series of measurements with a stationary tag. The tag was placed at a set of calibration points, surveyed to 5 mm accuracy and covering the working space. We aligned tag's orientation with that of the anchors, and all coordinates were taken of the same point on the modules' cases. For each point, we collected 5 s of DS-TWR ranges at 40 Hz, ran the 3-D EKF, and then compared the EKF-estimated position with the ground truth. The partial results are summarized in the table 1. The spatial distribution shows that positioning errors remain below 12 cm with occasional spikes up to 45 cm. We attribute this error to the presence of numerous signal reflectors within the laboratory environment, such as metallic objects and individuals.

Second, to determine the system's performance in processing dynamic motion, we conducted a series of experiments where the tag was attached to a pendulum with a measured length in one of the spots with a small positioning error. We used lengths in the range from 30 cm to 1.5 meters. For every pendulum length, we estimated the period of the oscillations using the EKF-filtered data and compared it with the theoretical value $T_p = 2\pi\sqrt{L_p/g}$. We've repeated some of the experiments using different oscillation planes. The values agreed to within 6% even for the experiment with horizontal pendulum amplitude A_p smaller than the overall positioning accurancy (< 8 cm, see the table 2 and fig. 8).

Spot	Ground truth [cm]	EKF mean [cm]	Error [cm]
1	(3.00, 0.21, 0.74)	(3.10, 0.21, 0.74)	10
2	(0.90, 3.00, 0.00)	(0.85, 3.01, 0.07)	9
3	(3.90, 0.88, 1.77)	(3.91, 0.76, 1.75)	12
4	(1.94, 1.50, 0.76)	(1.70, 1.40, 0.94)	31
5	(3.30, 3.30, 0.00)	(3.15, 3.70, 0.15)	45
6	(3.60, 3.40, 1.00)	(3.57, 3.33, 1.07)	10

Table 1. Coordinate comparison at six representative spots

L_p [cm]	A_p [cm]	F_p [Hz]	$\hat{f}_{\text{EKF}}$ [Hz]	ϵ_{rel} [%]
150	30, X	0.406	0.401	1.2
150	30, Y	0.406	0.405	0.2
94	20, X	0.513	0.498	2.9
94	20, Y	0.513	0.501	2.3
31	8, X	0.895	0.847	5.3

Table 2. Theoretical F_p and measured $\hat{f}_{\text{EKF}}$ frequency of a pendulum with different suspension length L_p and initial horizontal amplitude A_p

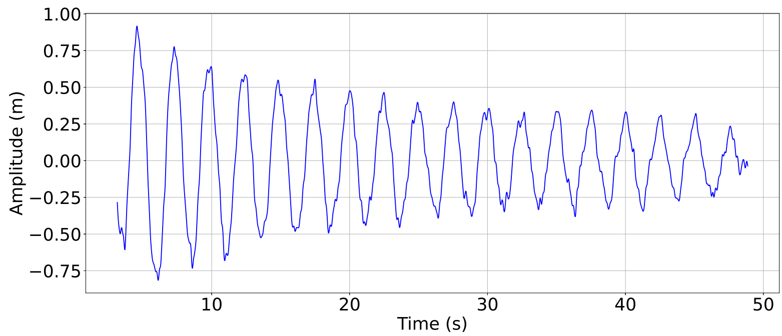

Figure 8. Estimated tag displacement during the pendulum experiment. (L_p=1.5 m)

Conclusions

.

The presented course enables students to develop skills in conducting experimental work using UWB electronic equipment. Methods of statistics and Kalman filtering are used to process the experimental results, allowing to obtain positioning accuracy of 12 centimeters under the lab conditions. Consequently, students will gain experience in using MicroPython to work with UWB devices. This laboratory course could be integrated as experimental part into courses on electronics, radioengineering, and antennas.

This laboratory exercise can be valuable for curricula aimed at training specialists in unmanned systems and robotics.

The presented laboratory course has been piloted as a training program for students at Moscow Institute of Physics and Technology.

References

[1] International Telecommunication Union Radiocommunication Sector (ITU-R), Recommendation ITU-R SM.1755-0, International Telecommunication Union, Geneva, Switzerland (2006), https://www.intertekinform.com/en-us/standards/itu-r-sm-1755-0-05-2006–1219215_saig_itu_itu_2959840/

[2] Z. Xiang, L. Chen, Q. Wu, J. Yang, X. Dai, X. Xie, An improved UWB indoor positioning approach for UAVs based on the dual-anchor model, Sensors **25** (2025). 10.3390/s25041052

[3] SW-DWM1001-Firmware-User-Guide-1.4, DWM1001 Firmware User Guide, Decawave (2017)

[4] J. Qiao, F. Yang, J. Liu, G. Huang, W. Zhang, M. Li, Advancements in indoor precision positioning: A comprehensive survey of UWB and Wi-Fi RTT Positioning Technologies, Network **4**, 545 (2024). 10.3390/network4040027

[5] G. Deak, K. Curran, J. Condell, A survey of active and passive indoor localisation systems, Computer Communications **35**, 1939 (2012). https://doi.org/10.1016/j.comcom.2012.06.004

[6] M.F.R. Al-Okby, S. Junginger, T. Roddelkopf, K. Thurow, UWB-based real-time indoor positioning systems: A comprehensive review, Applied Sciences **14** (2024). 10.3390/app142311005

[7] D. Coppens, A. Shahid, S. Lemey, B. Van Herbruggen, C. Marshall, E. De Poorter, An overview of UWB standards and organizations (ieee 802.15.4, FiRa, apple): Interoperability aspects and future research directions, IEEE Access **10**, 70219 (2022). 10.1109/ACCESS.2022.3187410

[8] A. Volpi, L. Tebaldi, G. Matrella, R. Montanari, E. Bottani, Low-cost UWB based real-time locating system: Development, lab test, industrial implementation and economic assessment, Sensors **23** (2023). 10.3390/s23031124

[9] N.H.H. Pham, M.A. Nguyen, C.C. Sun, Indoor Positioning System using UWB and Kalman filter to increase the accuracy of the Localization System, in *2022 IEEE International Conference on Consumer Electronics - Taiwan* (2022), pp. 339–340

[10] Y. Zeng, S. Shen, Eliminating UWB Self Positioning Error Based on Kalman Filter Algorithm, in *Proceedings of the 2022 2nd International Conference on Bioinformatics and Intelligent Computing* (Association for Computing Machinery, New York, NY, USA, 2022), BIC '22, p. 217–222, ISBN 9781450395755, `https://doi.org/10.1145/3523286.3524544`

[11] Y. Hu, X. Zhao, UWB Localization Algorithm Based on Kalman Filter and IPSO Algorithm, in *2024 12th International Conference on Information Systems and Computing Technology (ISCTech)* (2024), pp. 1–5

[12] E. Dehmollaian, B. Etzlinger, P. Peterseil, A. Springer, AI-Enhanced UWB-Based Localisation in Wireless Networks (Springer Nature Switzerland, Cham, 2024), pp. 201–216, ISBN 978-3-031-54049-3, doi:10.1007/978-3-031-54049-3-12

[13] G. Welch, G. Bishop, An Introduction to the Kalman Filter (University of North Carolina at Chapel Hill, USA, 1995)

[14] J. Sidorenko, V. Schatz, N. Scherer-Negenborn, M. Arens, U. Hugentobler, Decawave ultra-wideband warm-up error correction, IEEE Transactions on Aerospace and Electronic Systems **57**, 751 (2020).

[15] J. Dong, Z. Lian, J. Xu, Z. Yue, Uwb localization based on improved robust adaptive cubature kalman filter, Sensors **23**, 2669 (2023).

[16] J. Cano, G. Pages, E. Chaumette, J. LeNy, Clock and power-induced bias correction for uwb time-of-flight measurements, IEEE Robotics and Automation Letters **7**, 2431 (2022).

[17] C. Wang, H. Han, J. Wang, H. Yu, D. Yang, A robust extended kalman filter applied to ultrawideband positioning, Mathematical Problems in Engineering **2020**, 1809262 (2020).

[18] R.B. Langley et al., Dilution of precision, GPS world **10**, 52 (1999).

[19] J. Cho, S. Jeong, B. Lee, A study on anchor placement and 3d positioning algorithm for UWB application in small sites, KSCE Journal of Civil Engineering **28**, 4575 (2024).

[20] J. Cho, B. Lee, Optimal layout of four anchors to improve accuracy of ultra-wide band based indoor positioning, Expert Systems with Applications **255**, 124808 (2024).